Journal of
Mechanics of
Materials and Structures

ELECTROELASTIC INTENSIFICATION AND DOMAIN SWITCHING NEAR A PLANE STRAIN CRACK IN A RECTANGULAR PIEZOELECTRIC MATERIAL

Yasuhide Shindo, Fumio Narita and Fumitoshi Saito

Volume 2, Nº 8 October 2007

mathematical sciences publishers

JOURNAL OF MECHANICS OF MATERIALS AND STRUCTURES
Vol. 2, No. 8, 2007

ELECTROELASTIC INTENSIFICATION AND DOMAIN SWITCHING NEAR A PLANE STRAIN CRACK IN A RECTANGULAR PIEZOELECTRIC MATERIAL

YASUHIDE SHINDO, FUMIO NARITA AND FUMITOSHI SAITO

We study the effects of crack face boundary conditions and localized polarization switching on the piezoelectric fracture. This paper consists of two parts. In the first part, the electroelastic problem of an infinite piezoelectric material with a crack is formulated by means of integral transforms, and the exact solution is obtained. The electroelastic fields are expressed in closed form. The fracture mechanics parameters, such as energy release rate, are obtained for the permeable, impermeable and open crack models. In the second part, finite element analysis is carried out to study the crack behavior in a rectangular piezoelectric material by introducing a model for polarization switching in local areas of electroelastic field concentrations. A nonlinear behavior induced by localized polarization switching is observed between the fracture mechanics parameters and applied electric field.

1. Introduction

The fracture behavior of piezoelectric materials has received much attention in recent years. In the theoretical studies of the piezoelectric crack problems, there are two commonly used electrical boundary conditions across the crack face: (1) the permeable crack model and (2) the impermeable crack model. Theoretical analyses on cracked piezoelectric ceramics indicated that a negative energy release rate is produced for the impermeable crack model [Narita et al. 2003]. Furthermore, some experimental results show that the fracture loads are increased or decreased depending on the mechanical loading conditions (applied load or applied displacement) and direction of electric fields [Park and Sun 1995; Shindo et al. 2002; Narita et al. 2003; Shindo et al. 2005]. These experimentally observed phenomena contradict the results of the calculations using energy release rate for the impermeable crack model. Recently, some researchers [Xu and Rajapakse 2001; Wang and Mai 2003; Landis 2004; McMeeking 2004] used the open piezoelectric crack model [Hao and Shen 1994] and discussed the effect of electric fields on the fracture mechanics parameters such as energy release rate. Although the impermeable and open crack models may provide mathematical solutions of piezoelectric cracks, there is still a great deal of uncertainty in searching for fracture design parameters characterizing the electric failure.

The nonlinear effect caused by the polarization switching may affect the piezoelectric fracture behavior [Fu and Zhang 2000; Shindo et al. 2003]. In this investigation, the effects of crack face boundary conditions and localized polarization switching near the crack tip on the piezoelectric fracture mechanics parameters are studied by analyzing the plane strain electroelastic problem of a piezoelectric material with a crack. First, the crack problem of an infinite piezoelectric material is formulated by means of

Keywords: elasticity, finite element method, piezoelectric material, crack, energy release rate, polarization switching.
This work was supported by the Ministry of Education, Culture, Sports, Science and Technology of Japan under the Grant-in-Aid for Scientific Research (B).

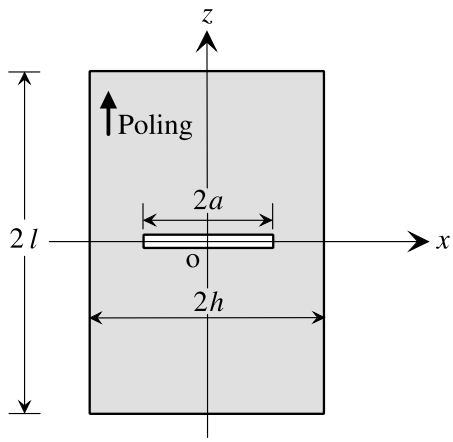

Figure 1. A rectangular piezoelectric material with a crack.

integral transforms and the solutions are obtained exactly. Electroelastic fields and energy release rate based on permeable, impermeable and open crack models are compared. Secondly, a finite element method incorporating the polarization switching mechanism is used to calculate the energy release rate in a rectangular piezoelectric material. The numerical results illustrate that the impermeable and open crack models can lead to significant errors regarding the effect of electric fields on piezoelectric crack propagation.

2. Statement of the problem and basic equations

A rectangular piezoelectric material of length $2l$ and width $2h$ contains a central crack of length $2a$, as shown in Figure 1. A set of Cartesian coordinates $\{x, y, z\}$ is attached to the center of the crack normal to the z-axis. The piezoelectric material has symmetry properties of hexagonal crystal of 6 mm class with respect to the x, y, z-axes, and is under a state of plane strain. The material is loaded by mechanical displacement u_0 with the electric field in the z-direction of the poling axis. Due to the symmetry of the problem, only the first quadrant with appropriate boundary conditions needs to be analyzed.

The constitutive equations can be written as

$$\sigma_{xx} = c_{11}u_{x,x}+c_{13}u_{z,z}-e_{31}E_z, \quad \sigma_{zx} = c_{44}(u_{x,z}+u_{z,x})-e_{15}E_x, \quad \sigma_{zz} = c_{13}u_{x,x}+c_{33}u_{z,z}-e_{33}E_z, \tag{1}$$

$$D_x = e_{15}(u_{x,z}+u_{z,x})+\epsilon_{11}E_x, \quad D_z = e_{31}u_{x,x}+e_{33}u_{z,z}+\epsilon_{33}E_z. \tag{2}$$

Here $\sigma_{xx}, \sigma_{zz}, \sigma_{xz} = \sigma_{zx}$ are the components of stress tensor, D_x and D_z are the components of electric displacement vector, u_x and u_z are the components of displacement vector, E_x and E_z are the components of electric field intensity vector; $c_{11}, c_{13}, c_{33}, c_{44}$ are the elastic stiffness constants measured in a constant electric field, $\epsilon_{11}, \epsilon_{33}$ are the dielectric permittivities measured at constant strain, and e_{15}, e_{31}, e_{33} are the piezoelectric constants. A comma implies partial differentiation with respect to the coordinates. The electric field components are related to the electric potential $\phi(x, z)$ via $E_x = -\phi_{,x}$ and $E_z = -\phi_{,z}$. The

governing equations can be written as

$$\begin{aligned} c_{11}u_{x,xx} + c_{44}u_{x,zz} + (c_{13}+c_{44})u_{z,xz} + (e_{31}+e_{15})\phi_{,xz} &= 0,\\ c_{44}u_{z,xx} + c_{33}u_{z,zz} + (c_{13}+c_{44})u_{x,xz} + e_{15}\phi_{,xx} + e_{33}\phi_{,zz} &= 0,\\ (e_{31}+e_{15})u_{x,xz} + e_{15}u_{z,xx} + e_{33}u_{z,zz} - \epsilon_{11}\phi_{,xx} - \epsilon_{33}\phi_{,zz} &= 0. \end{aligned} \tag{3}$$

In a vacuum, the constitutive equations (2) and the governing equation $(3)_3$ become

$$D_x = \epsilon_0 E_x, \qquad D_z = \epsilon_0 E_z, \qquad \phi_{,xx} + \phi_{,zz} = 0, \tag{4}$$

where $\epsilon_0 = 8.85 \times 10^{-12}$ C/Vm is the electric permittivity of the vacuum.

The crack face boundary and the loading conditions can be expressed in the form

$$\sigma_{zx}(x,0) = 0 \quad (0 \le x \le h), \qquad \sigma_{zz}(x,0) = 0 \quad (0 \le x < a), \qquad u_z(x,0) = 0 \quad (a \le x \le h) \tag{5}$$

$$E_x(x,0) = E_x^c(x,0) \quad (0 \le x < a), \qquad \phi(x,0) = 0 \quad (a \le x \le h), \tag{6}$$

$$D_z(x,0) = D_z^c(x,0) \quad (0 \le x < a), \tag{7}$$

$$u_z(x,l) = u_0, \quad (0 \le x \le h), \phi(x,l) = \phi_0 \quad (0 \le x \le h). \tag{8}$$

where ϕ_0 is an applied electric potential and the superscript c stands for the electric field quantity in the void inside the crack. The electric potential is zero on the symmetry planes inside the crack and ahead of the crack, so the boundary conditions (6) reduce to $\phi(x,0) = 0$ for $0 \le x \le h$. Equations (6) and (7) are the permeable boundary conditions.

Applying the loading conditions (8), the stress σ_{zz} for the uncracked piezoelectric material is

$$\sigma_{zz}(x,z) = \sigma_0 - e_1 E_0, \qquad \sigma_0 = \left(c_{33} - \frac{c_{13}^2}{c_{11}}\right)\frac{u_0}{l}, \qquad E_0 = -\frac{\phi_0}{l}, \qquad e_1 = e_{33} - \left(\frac{c_{13}}{c_{11}}\right)e_{31}. \tag{9}$$

The stress at $z = l$ for the uncracked piezoelectric material is denoted by $\sigma_l = \sigma_0 - e_1 E_0$. Note that σ_0 is the stress for a closed-circuit condition with the potential forced to remain zero (grounded) and depends only on the displacement at the edge $z = l$. When a uniform displacement u_0 is applied and fixed at $z = l$, the stress σ_0 will be uniform. On the other hand, when the stress σ_l is applied and fixed at $z = l$, σ_l is left unchanged and the displacement u_0 depends on E_0.

3. Cracked infinite piezoelectric material

In this section we consider the problem of an infinite piezoelectric material with a crack for $l \to \infty$ and $h \to \infty$. The material is under applied uniform strain ε_0 and electric field E_0 at infinity. The stress at infinity is denoted by $\sigma_l = \sigma_0 - e_1 E_0$, and Equation $(9)_2$ can be rewritten in terms of ε_0 as $\sigma_0 = \left(c_{33} - c_{13}^2/c_{11}\right)\varepsilon_0$. Fourier transforms are used to reduce the mixed boundary value problem to a pair of dual integral equations. The integral equations then can be solved exactly; see Appendix A. The energy release rate G for the permeable crack model may be expressed as

$$G = \frac{1}{2F^2}\left(- F\sum_{j=1}^{3}\frac{d_j}{\gamma_j} + \sum_{k=1}^{3} h_k d_k \sum_{j=1}^{3}\frac{b_j d_j}{\gamma_j}\right) K_{\mathrm{I}}^2, \tag{10}$$

where the stress intensity factor K_{I} is defined as $K_{\mathrm{I}} = \lim_{x\to a^+}[2\pi(x-a)]^{1/2}\sigma_{zz}(x,0)$. The stress intensity factor under applied strain and applied stress is given by, respectively,

$$K_{\mathrm{I}} = \left\{\left(c_{33} - \frac{c_{13}^2}{c_{11}}\right)\varepsilon_0 - e_1 E_0\right\}(\pi a)^{1/2}, \qquad K_{\mathrm{I}} = \sigma_l(\pi a)^{1/2}. \tag{11}$$

Energy release rates for the impermeable and open crack models are discussed in Appendices B and C, respectively.

4. Cracked rectangular piezoelectric material

In this section the finite element computer program ANSYS is selected for the analysis of the configuration considered here. A nonlinear finite element model incorporating the polarization switching mechanisms with the energy release rate calculations is developed. Two criteria are used for this purpose: work done switching criterion, and internal energy density switching criterion.

The first criterion requires that a polarization switches when the combined electrical and mechanical work exceeds a critical value [Hwang et al. 1995]

$$\sigma_{xx}\Delta\varepsilon_{xx} + \sigma_{zz}\Delta\varepsilon_{zz} + 2\sigma_{zx}\Delta\varepsilon_{zx} + E_x\Delta P_x + E_z\Delta P_z = 2P^{\mathrm{s}}E_{\mathrm{c}}, \tag{12}$$

where $\Delta\varepsilon_{xx}$, $\Delta\varepsilon_{zz}$, $\Delta\varepsilon_{zx}$ are the changes in the spontaneous strain γ^{s}, ΔP_x, ΔP_z are the changes in the spontaneous polarization P^{s}, and E_{c} is a coercive electric field. It is assumed that elastic and dielectric constants of the piezoelectric materials remain unchanged after 180° or 90° polarization switching occurs and only piezoelectric constants vary with switching. It is also assumed that for 90° switching there are two allowable directions of the poling in the coordinate system: in the positive and negative x-direction. The changes in spontaneous strains and polarizations for 180° switching can be expressed as

$$\Delta\varepsilon_{xx} = \Delta\varepsilon_{zz} = \Delta\varepsilon_{zx} = 0, \qquad \Delta P_x = 0, \qquad \Delta P_z = -2P^{\mathrm{s}}.$$

For 90° switching in the xz plane, we have

$$\Delta\varepsilon_{xx} = \gamma^{\mathrm{s}}, \qquad \Delta\varepsilon_{zz} = -\gamma^{\mathrm{s}}, \qquad \Delta\varepsilon_{zx} = 0, \qquad \Delta P_x = \pm P^{\mathrm{s}}, \qquad \Delta P_z = -P^{\mathrm{s}}.$$

The polarization switching criterion based on internal energy density is defined as [Sun and Achuthan 2004]

$$U = U_{\mathrm{c}}, \tag{13}$$

where U is the internal energy density and U_c is its critical value corresponding to the switching mode. The internal energy density associated with 180° and 90° switching, respectively, is

$$U = \tfrac{1}{2}D_z E_z, \qquad U = \tfrac{1}{2}(\sigma_{xx}\varepsilon_{xx} + \sigma_{zz}\varepsilon_{zz} + 2\sigma_{zx}\varepsilon_{zx} + D_x E_x).$$

We assume that the critical value of internal energy density takes the form $U_{\mathrm{c}} = \frac{1}{2}\epsilon_{33}^{\mathrm{T}}(E_{\mathrm{c}})^2$, where $\epsilon_{33}^{\mathrm{T}}$ is the dielectric permittivity at constant stress.

Due to polarization switching, piezoelectric materials are often nonhomogeneous. The piezoelectric properties vary from one location to the other, and the variations are either continuous or discontinuous.

The energy release rate G can be obtained from the following crack tip integral [Shindo et al. 2005]:

$$G = \left(\int_{\Gamma_0} - \int_{\Gamma_p} \right) \{ H n_x - (\sigma_{xx} u_{x,x} + \sigma_{zx} u_{z,x}) n_x - (\sigma_{zx} u_{x,x} + \sigma_{zz} u_{z,x}) n_z + D_x E_x n_x + D_z E_x n_z \} d\Gamma,$$

where Γ_0 is a small contour closing a crack tip, Γ_p is a path embracing that part of phase boundary which is enclosed by Γ_0, and n_x, n_z are the components of the outer unit normal vector. The electrical enthalpy density H is

$$H(u_x, u_z, E_x, E_z) = \tfrac{1}{2}\left(c_{11} u_{x,x}^2 + c_{33} u_{z,z}^2 + 2c_{13} u_{x,x} u_{z,z} + c_{44}(u_{x,z} + u_{z,x})^2\right) - \left[\tfrac{1}{2}\left(\epsilon_{11} E_x^2 + \epsilon_{33} E_z^2\right) + e_{15}(u_{x,z} + u_{z,x}) E_x + (e_{31} u_{x,x} + e_{33} u_{z,z}) E_z\right].$$

Each element consists of many grains, and each grain is modeled as a uniformly polarized cell that contains a single domain. The model neglects the domain wall effects and interaction among different domains. In reality these effects matter, but the assumption does not affect the general conclusions drawn. The polarization of each grain initially aligns as closely as possible to the z-direction. Polarization switching is defined for each element in the material. The displacement u_0 and electric potential ϕ_0 are applied at the edge $0 \le x \le h$, $z = l$, and the electroelastic fields of each element are computed from the finite element analysis. The switching criterion (12) or (13) is checked for every element to see if switching will occur. After all possible polarization switches have occurred, the piezoelectric tensor of each element is rotated to the new polarization direction. The electroelastic fields are recalculated, and the process is repeated until the solution converges. The macroscopic response of the material is determined by the finite element model, which is an aggregate of elements. The spontaneous polarization P^s and strain γ^s are assigned representative values of 0.3 C/m^2 and 0.004, respectively. Our previous experiments [Yoshida et al. 2003; Shindo et al. 2004; Narita et al. 2005] verified the accuracy of the above scheme, and showed that the results obtained are of general applicability. After polarization switching is predicted, J-integral paths are selected, which do not pass exactly through the singular point.

The calculations of the electroelastic fields and energy release rate for the open crack model are more complicated than for the permeable and impermeable crack models. The open crack model calculations start with $\phi = 0$ on the crack surface [McMeeking 1999]. The crack opening displacement and charge density on the crack surface are estimated, and the resulting potential difference is applied to the crack surface. The electroelastic fields are again solved leading to new crack opening displacement and charge density on the crack surface. If this is accomplished, then the potential difference is applied once more to the crack surface. Such a procedure is repeated until the evolution of the objective solutions shows no improvements.

5. Numerical results and discussion

Numerical calculations have been carried out for commercially available piezoelectric ceramics C-91 (Fuji Ceramics, Japan). The material properties of C-91 are listed in Table 1, and the coercive electric field E_c is approximately 0.35 MV/m. Figure 2a shows the crack opening displacement $u_z(x, 0^+)$ from the theoretical solutions for an infinite C-91 ($l, h \to \infty$) with a crack of length $2a = 2$ mm under $\varepsilon_0 = 5 \times 10^{-5}$ and $E_0 = 0$. The results for the permeable, open and impermeable crack models are shown

Elastic stiffnesses ($\times 10^{10}$ N/m^2)					Piezoelectric coefficients (C/m^2)			Dielectric constants ($\times 10^{-10}$ C/V m)	
c_{11}	c_{12}	c_{13}	c_{33}	c_{44}	e_{31}	e_{33}	e_{15}	ϵ_{11}	ϵ_{33}
12.0	7.7	7.7	11.4	2.4	−17.3	21.2	20.2	226	235

Table 1. Material properties of C-91.

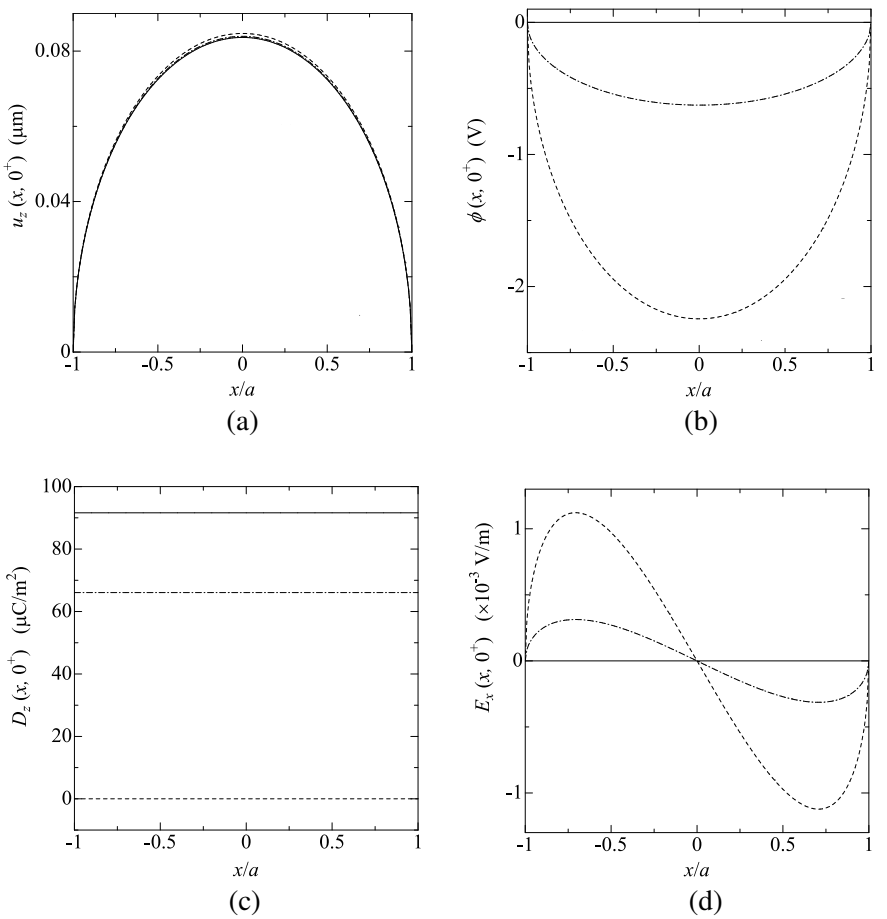

Figure 2. (a) Displacement $u_z(x, 0^+)$; (b) electric potential $\phi(x, 0^+)$; (c) normal component of electric displacement $D_z(x, 0^+)$; and (d) tangential component of electric field $E_x(x, 0^+)$ along the upper crack surface for an infinite piezoelectric material C-91 under uniform strain. Here $l, h \to \infty$, $a = 1$ mm, $\varepsilon_0 = 5 \times 10^{-5}$ and $E_0 = 0$. The permeable model is represented by the solid line, open by the dot-dashed line, and the impermeable by the dashed line.

for comparison purposes. Little difference among three piezoelectric crack models is observed. The rest of Figure 2 shows the electric potential $\phi(x, 0^+)$, normal component of electric displacement $D_z(x, 0^+)$ and tangential component of electric field $E_x(x, 0^+)$ along the upper crack surface. There are differences among the crack models. It is noted that the open and impermeable crack models reduce the continuity of the tangential components of the electric field across the crack surface.

Figure 3a presents the crack opening displacement $u_z(0, 0^+)$ at the center of the crack versus electric field E_0 from the finite element analysis without the polarization switching effect. The rectangular piezoelectric material C-91 with a crack of length $2a = 2\,\text{mm}$ has a length $2l = 20\,\text{mm}$ and width $2h = 20\,\text{mm}$, and is under applied displacement $u_0 = 0.5\,\mu\text{m}$ corresponding to the uniform strain 5×10^{-5} for the uncracked material. For comparison, the results for the infinite piezoelectric material ($l, h \to \infty$, $\varepsilon_0 = 5 \times 10^{-5}$) obtained from the theoretical analysis are included. The results for the finite element analysis agree with the theoretical analysis data. Figure 3b shows similar results for the normal component of electric displacement $D_z(0, 0^+)$.

Figure 4a shows the dependence of the energy release rate G on E_0. The results for the infinite piezoelectric material obtained from the theoretical analysis are also shown. The energy release rates are lower for positive electric fields and higher for negative electric fields under applied displacement. In the impermeable case, a negative energy release rate is produced. The energy release rate for the permeable crack in the infinite piezoelectric material under applied stress is independent of the electric field (not shown). Figure 4b shows the similar results under $u_0 = 1\,\mu\text{m}$ with $\varepsilon_0 = 10^{-4}$. A negative energy release rate is also produced for the open crack model. The parameters for the impermeable and open crack models have questionable physical significance.

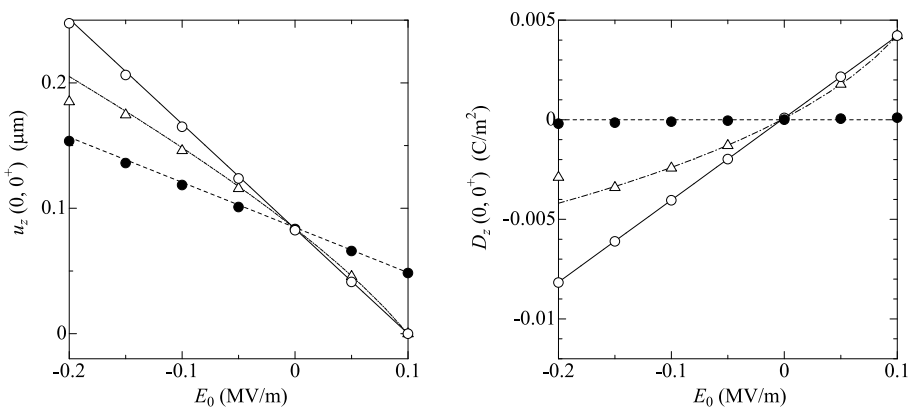

Figure 3. (a) Crack center displacement $u_z(0, 0^+)$ and (b) normal component of electric displacement $D_z(0, 0^+)$ versus electric field E_0 for rectangular piezoelectric material C-91 under applied displacement for finite element analysis data $l = h = 10\,\text{mm}$, whereas the theoretical prediction is made with $l, h \to \infty$. $a = 1\,\text{mm}$, $\varepsilon_0 = 5 \times 10^{-5}$, and $u_0 = 0.5\,\mu\text{m}$. The permeable theory is represented by the solid line and data with open circles, open by the dot-dashed line and triangles, and the impermeable by the dashed line and solid circles.

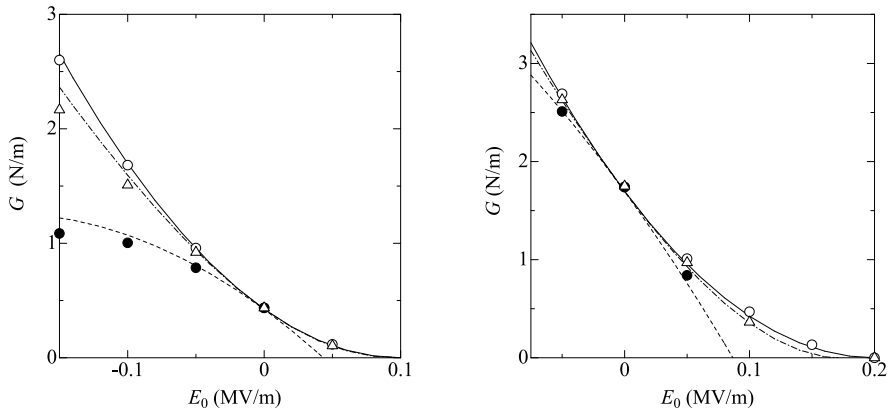

Figure 4. Energy release rate G versus electric field E_0 for rectangular piezoelectric material C-91 under applied displacement. For finite element analysis data $l = h = 10\,\text{mm}$, whereas the theoretical prediction is made with $l, h \to \infty$; also $a = 1\,\text{mm}$. (a) $\varepsilon_0 = 5 \times 10^{-5}$ and $u_0 = 0.5\,\mu\text{m}$, (b) $\varepsilon_0 = 10^{-4}$ and $u_0 = 1\,\mu\text{m}$. For legend, see Figure 3.

Figure 5 displays the variation of G with electric field E_0 for the permeable crack model from the finite element analysis with and without the polarization switching effect. For the polarization switching effect, the predictions by the criteria based on work (12) and energy density (13) are shown. The rectangular piezoelectric material C-91 ($2l = 5\,\text{mm}$, $2h = 5\,\text{mm}$) with a crack ($2a = 2\,\text{mm}$) is under applied displacement $u_0 = 0.125\,\mu\text{m}$ corresponding to the uniform strain 5×10^{-5} for the uncracked material. Positive electric fields decrease the values of G, while negative electric fields have an opposite effect. A monotonically increasing negative E_0 causes polarization switching. The value of electric field associated with the switching is $-0.25\,\text{MV/m}$ for the work-based criterion, while it is approximately $-0.17\,\text{MV/m}$ for

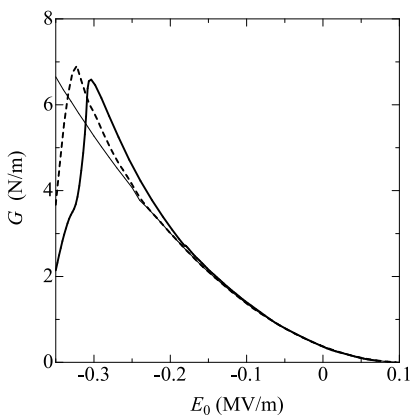

Figure 5. Energy release rate G versus electric field E_0 for rectangular piezoelectric material C-91 under applied displacement in the permeable model. $l = h = 2.5\,\text{mm}$, $a = 1\,\text{mm}$, and $u_0 = 0.125\,\mu\text{m}$. Thin line gives prediction without polarization switching; the dashed line gives work-based and thick line gives energy density-based switching effect.

the criterion based on the energy density. When the negative E_0 increases further, G with the polarization switching effect becomes larger than that without the switching effect. After E_0 reaches about -0.325 (-0.305) MV/m, polarization switching in a local region, based on the work (energy density), leads to an unexpected decrease in G for the permeable crack. Our previous experimental study [Shindo et al. 2003] showed a significant nonlinearity in the fracture load due to polarization switching. The nonlinear effect caused by polarization switching may affect the piezoelectric crack behavior.

Figure 6 shows the 180° and 90° switching zones near the permeable crack tip in the rectangular piezoelectric material C-91 ($2l = 5$ mm, $2h = 5$ mm, $2a = 2$ mm) under $u_0 = 0.125\,\mu$m for various values of E_0. Predictions resulting from different criteria are presented. The size of the 180° (90°) switching zone behind (ahead of) the crack tip increases at first when the negative E_0 is increased, and the difference between energy release rate results with and without switching effect becomes larger at a higher negative E_0. As the negative E_0 continues increasing, the area of the 180° switching zone grows ahead of the crack tip. Unexpected decrease in G is attributed to 180° switching ahead of the crack tip. In the impermeable case, the region ahead of the crack tip is found to undergo 180° switching due to the large negative electric field, and the region behind the crack tip has 90° switching because of the large intensified electric field E_x [Kalyanam and Sun 2005].

The applied displacement may enhance the polarization switching depending on its magnitude. The critical value of the electric field associated with the polarization switching decreases (relative to $u_0 =$

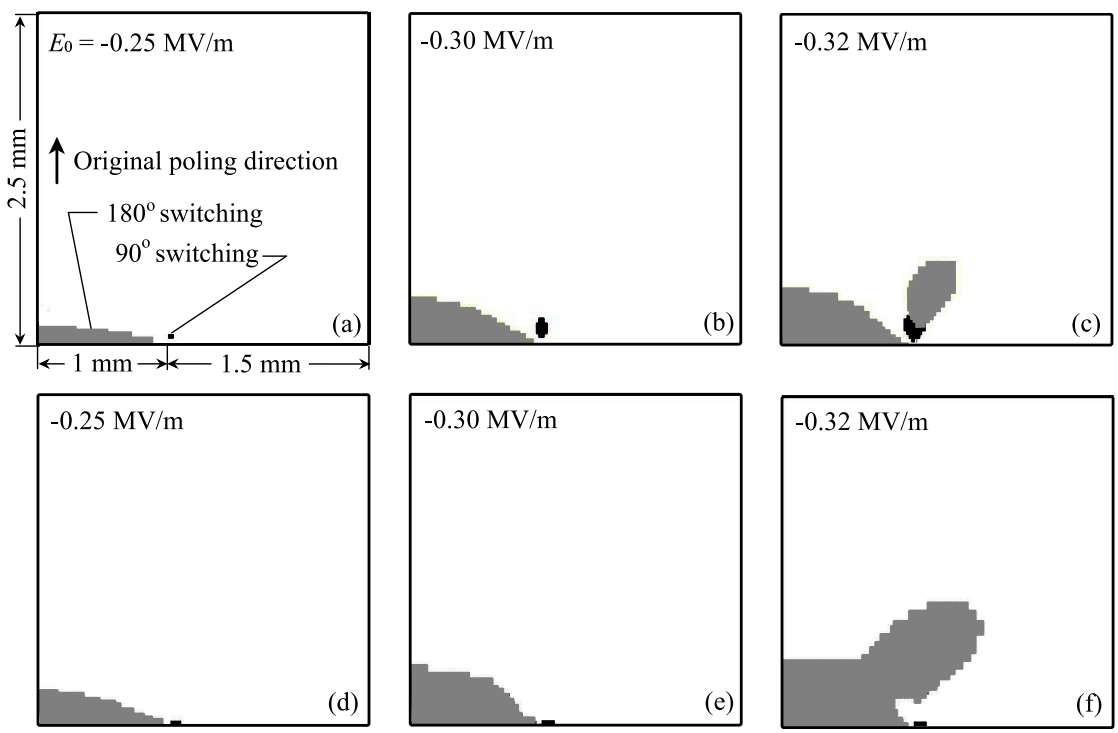

Figure 6. Polarization switching zone induced by displacement $u_0 = 0.125\,\mu$m and electric field E_0 of (a, d) -0.25, (b, e) -0.30, (c, f) -0.32 MV/m based on different criteria: (a–c) work and (d–f) energy density.

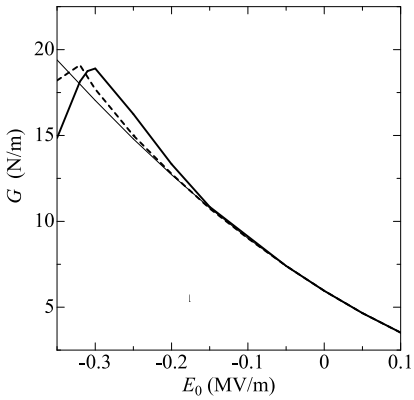

Figure 7. Energy release rate G versus electric field E_0 for rectangular piezoelectric material C-91 under applied displacement in the permeable model. $l = h = 2.5$ mm, $a = 1$ mm, and $u_0 = 0.5\ \mu$m. For legend, see Figure 5.

0.125 μm) when $u_0 = 0.5\ \mu$m is applied, as shown in Figure 7. After E_0 reaches about -0.21 (-0.15) MV/m, the G with the switching effect, based on the work (energy density), deviates from the curve without the switching effect. This is due to the 180° switching behind the crack tip; see Figure 8. As

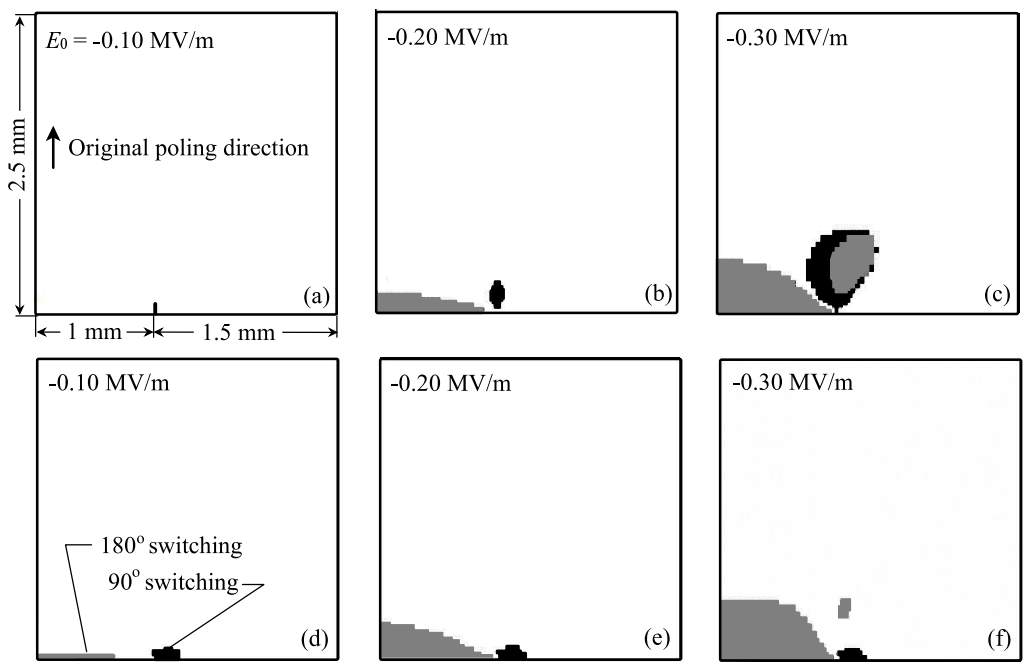

Figure 8. Polarization switching zone induced by displacement $u_0 = 0.5\ \mu$m and electric field E_0 of (a, d) -0.10, (b, e) -0.20, (c, f) -0.30 MV/m based on different criteria: (a–c) work; (d–f) energy density.

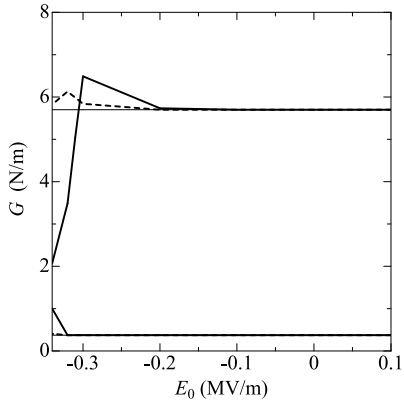

Figure 9. Energy release rate G versus electric field E_0 for rectangular piezoelectric material C-91 under applied stress in the permeable model. $l = h = 2.5$ mm and $a = 1$ mm. We present results for $\sigma_l = 22.8$ and 5.70 MPa. For legend, see Figure 5.

E_0 reaches about -0.32 (-0.30) MV/m, G falls. In the experimental data [Sun and Park 2000], crack length deviated from the linear function of the electric field for the case of a larger load, especially for negative electric fields. By including the polarization switching effect of the energy release rate, the observed nonlinear dependence of piezoelectric crack behavior on the electric field is explained.

Figure 9 shows the energy release rate G versus electric field E_0 under applied stress. The rectangular piezoelectric material C-91 ($2l = 5$ mm, $2h = 5$ mm) with a permeable crack ($2a = 2$ mm) is subjected to the stress $\sigma_l = 22.8$ MPa, corresponding to the uniform strain 2×10^{-4} for the uncracked material without the electric field. We also present data for $\sigma_l = 5.70$ MPa. The results for positive E_0 under applied stress are different from those under applied displacement, and the energy release rate for the permeable crack in the rectangular piezoelectric material is independent of the positive E_0. The behavior of the energy release rate for negative E_0 is complicated because of the polarization switching phenomena.

6. Conclusions

Theoretical and finite element analyses are presented for the cracked piezoelectric materials under tension. Based on the results of this study, the following conclusions may be inferred:

(1) Piezoelectric crack face boundary conditions strongly affect the electric field effect characteristics of the electromechanical behavior and fracture mechanics parameters such as energy release rate.

(2) The energy release rate criteria for the open and impermeable crack models led to negative values which are unphysical. The energy release rate for the permeable crack always remains positive.

(3) For the permeable crack in the rectangular piezoelectric material, the positive electric field decreases the energy release rate under applied displacement. If the negative electric field is applied, localized polarization switching occurs due to electroelastic field concentrations near the crack tip, and the switching causes a sudden change in the energy release rate under applied displacement or stress.

(4) The higher mechanical loading level decreases the critical value of the electric field associated with the polarization switching, and the localized 180° switching ahead of the crack tip can significantly influence the energy release rate.

Appendix A

We consider an infinite piezoelectric material with a permeable crack under applied strain ε_0 and electric field E_0. The crack face boundary and loading conditions become

$$\sigma_{zx}(x,0)=0 \quad (0\le x<\infty), \qquad \sigma_{zz}(x,0)=0 \quad (0\le x<a), \qquad u_z(x,0)=0 \quad (a\le x<\infty), \tag{A.1}$$

$$E_x(x,0)=E_x^c(x,0) \quad (0\le x<a), \qquad \phi(x,0)=0 \quad (a\le x<\infty), \tag{A.2}$$

$$D_z(x,0)=D_z^c(x,0) \quad (0\le x<a), \tag{A.3}$$

$$\varepsilon_{zz}(x,z)=\varepsilon_0 \quad (0\le x<\infty, z\to\infty), \qquad E_z(x,z)=E_0 \quad (0\le x<\infty, z\to\infty). \tag{A.4}$$

Fourier transform is applied to Equations (3) and the results satisfying the loading conditions (A.4) are

$$\begin{aligned}
u_x(x,z)&=\frac{2}{\pi}\sum_{j=1}^{3}\int_0^\infty a_j A_j(\alpha)\exp(-\gamma_j\alpha z)\sin(\alpha x)d\alpha+\left(\frac{c_{13}}{c_{13}^2-c_{33}c_{11}}(\sigma_l+e_1E_0)+\frac{e_{31}}{c_{11}}E_0\right)x,\\
u_z(x,z)&=\frac{2}{\pi}\sum_{j=1}^{3}\int_0^\infty \frac{1}{\gamma_j}A_j(\alpha)\exp(-\gamma_j\alpha z)\cos(\alpha x)d\alpha+\frac{c_{11}}{c_{33}c_{11}-c_{13}^2}(\sigma_l+e_1E_0)z,\\
\phi(x,z)&=-\frac{2}{\pi}\sum_{j=1}^{3}\int_0^\infty \frac{b_j}{\gamma_j}A_j(\alpha)\exp(-\gamma_j\alpha z)\cos(\alpha x)d\alpha-E_0z,
\end{aligned} \tag{A.5}$$

where $A_j(\alpha)$ are the unknowns to be solved for, a_j and b_j stand for expressions

$$a_j=\frac{(e_{31}+e_{15})(c_{33}\gamma_j^2-c_{44})-(c_{13}+c_{44})(e_{33}\gamma_j^2-e_{15})}{(c_{44}\gamma_j^2-c_{11})(e_{33}\gamma_j^2-e_{15})+(c_{13}+c_{44})(e_{31}+e_{15})\gamma_j^2}, \qquad b_j=\frac{(c_{44}\gamma_j^2-c_{11})a_j+(c_{13}+c_{44})}{e_{31}+e_{15}},$$

and γ_j^2 are the roots of the characteristic equation $a_0\gamma^6+b_0\gamma^4+c_0\gamma^2+d_0=0$ with

$$\begin{aligned}
a_0&=c_{44}(c_{33}\epsilon_{33}+e_{33}^2), \qquad d_0=-c_{11}(c_{44}\epsilon_{11}+e_{15}^2),\\
b_0&=-2c_{44}e_{15}e_{33}-c_{11}e_{33}^2-c_{33}(c_{44}\epsilon_{11}+c_{11}\epsilon_{33})+\epsilon_{33}(c_{13}+c_{44})^2\\
&\qquad +2e_{33}(c_{13}+c_{44})(e_{31}+e_{15})-c_{44}^2\epsilon_{33}-c_{33}(e_{31}+e_{15})^2,\\
c_0&=2c_{11}e_{15}e_{33}+c_{44}e_{15}^2+c_{11}(c_{33}\epsilon_{11}+c_{44}\epsilon_{33})-\epsilon_{11}(c_{13}+c_{44})^2\\
&\qquad -2e_{15}(c_{13}+c_{44})(e_{31}+e_{15})+c_{44}^2\epsilon_{11}+c_{44}(e_{31}+e_{15})^2.
\end{aligned}$$

Application of the Fourier transform to Equation $(4)_3$ yields

$$\phi^c=\frac{2}{\pi}\int_0^\infty C(\alpha)\sinh(\alpha z)\cos(\alpha x)d\alpha, \qquad (0\le x<a),$$

where $C(\alpha)$ is also unknown.

By applying the crack face boundary conditions of Equations (A.1) and (A.2), the unknowns $A_j(\alpha)$ are related to the stress σ_l via

$$A_j(\alpha) = -\frac{\pi}{2}\frac{d_j}{F}\frac{aJ_1(a\alpha)}{\alpha}\sigma_l,$$

where $J_1(\,)$ is the order one Bessel function of the first kind and $F = \sum_{j=1}^{3} g_j d_j$ with

$$d_1 = \gamma_1(b_2 f_3 - b_3 f_2), \qquad d_2 = \gamma_2(b_3 f_1 - b_1 f_3), \qquad d_3 = \gamma_3(b_1 f_2 - b_2 f_1),$$
$$f_j = c_{44}(a_j\gamma_j^2 + 1) - e_{15}b_j, \qquad g_j = c_{13}a_j - c_{33} + e_{33}b_j.$$

The displacement u_z and electric potential ϕ on the crack surface are given by

$$u_z(x,0) = -\frac{b}{F}\sigma_l(a^2 - x^2)^{1/2}, \qquad \phi(x,0) = 0, \qquad b = b_1(f_2 - f_3) + b_2(f_3 - f_1) + b_3(f_1 - f_2).$$

The tangential component of electric field E_x and the normal component of electric displacement D_z on the crack surface are

$$E_x(x,0) = 0, \qquad D_z(x,0) = D_l - \frac{\sigma_l}{F}\sum_{j=1}^{3} h_j d_j,$$
$$D_l = \frac{e_{31}c_{13} - e_{33}c_{11}}{c_{13}^2 - c_{33}c_{11}}\sigma_0 + \left(\frac{e_{31}^2}{c_{11}} + \epsilon_{33}\right)E_0, \qquad h_j = e_{31}a_j - e_{33} - \epsilon_{33}b_j.$$

The displacement component u_z and electric potential ϕ near the crack tip can be written as

$$u_z = -\frac{K_{\mathrm{I}}}{F}\left(\frac{r}{\pi}\right)^{1/2}\sum_{j=1}^{3}\frac{d_j}{\gamma_j}\left[\left(\cos^2\theta + \gamma_j^2\sin^2\theta\right)^{1/2} - \cos\theta\right]^{1/2},$$
$$\phi = \frac{K_{\mathrm{I}}}{F}\left(\frac{r}{\pi}\right)^{1/2}\sum_{j=1}^{3}\frac{b_j d_j}{\gamma_j}\left[\left(\cos^2\theta + \gamma_j^2\sin^2\theta\right)^{1/2} - \cos\theta\right]^{1/2}, \tag{A.6}$$

where the polar coordinates r and θ are defined by $r = [(x-a)^2 + z^2]^{1/2}$, $\theta = \tan^{-1} z/(x-a)$. The singular parts of the stress σ_{zz} and electric displacement D_z in the neighborhood of the crack tip are

$$\sigma_{zz} = \frac{K_{\mathrm{I}}}{2F(\pi r)^{1/2}}\sum_{j=1}^{3} g_j d_j\left[\frac{\left(\cos^2\theta + \gamma_j^2\sin^2\theta\right)^{1/2} + \cos\theta}{\cos^2\theta + \gamma_j^2\sin^2\theta}\right]^{1/2},$$
$$D_z = \frac{K_{\mathrm{I}}}{2F(\pi r)^{1/2}}\sum_{j=1}^{3} h_j d_j\left[\frac{\left(\cos^2\theta + \gamma_j^2\sin^2\theta\right)^{1/2} + \cos\theta}{\cos^2\theta + \gamma_j^2\sin^2\theta}\right]^{1/2}. \tag{A.7}$$

By using the concept of crack closure energy and the asymptotic behavior of electroelastic fields near the crack tip illustrated in Equations (A.6) and (A.7), the energy release rate G in Equation (10) for the permeable crack model can be obtained.

Appendix B

A solution procedure for the impermeable crack model in the infinite piezoelectric material is outlined here. The crack face electric boundary condition for the impermeable crack model is

$$D_z(x,0)=0 \quad (0\le x<a), \qquad \phi(x,0)=0 \quad (a\le x<\infty). \tag{B.8}$$

The unknowns $A_j(\alpha)$ in Equations (A.5) can be found using the same approach as in the permeable case. By applying the crack face boundary conditions of Equations (A.1) and (B.8), the unknowns $A_j(\alpha)$ are related to σ_l and D_l as follows:

$$\begin{aligned}
&\frac{f_1}{\gamma_1}A_1(\alpha)+\frac{f_2}{\gamma_2}A_2(\alpha)+\frac{f_3}{\gamma_3}A_3(\alpha)=0,\\
&\frac{1}{\gamma_1}A_1(\alpha)+\frac{1}{\gamma_2}A_2(\alpha)+\frac{1}{\gamma_3}A_3(\alpha)=-\frac{\pi}{2F'}\frac{a}{\alpha}J_1(a\alpha)(F_{22}\sigma_l-F_{12}D_l),\\
&\frac{b_1}{\gamma_1}A_1(\alpha)+\frac{b_2}{\gamma_2}A_2(\alpha)+\frac{b_3}{\gamma_3}A_3(\alpha)=\frac{\pi}{2F'}\frac{a}{\alpha}J_1(a\alpha)(F_{21}\sigma_l-F_{11}D_l).
\end{aligned}$$

where

$$F_{11}=\frac{1}{b}\sum_{j=1}^{3}g_jd_j, \qquad F_{12}=\frac{1}{b}\sum_{j=1}^{3}g_jl_j, \qquad F_{21}=\frac{1}{b}\sum_{j=1}^{3}h_jd_j, \qquad F_{22}=\frac{1}{b}\sum_{j=1}^{3}h_jl_j,$$

$$F'=F_{11}F_{22}-F_{12}F_{21}, \qquad l_1=\gamma_1(f_2-f_3), \qquad l_2=\gamma_2(f_3-f_1), \qquad l_3=\gamma_3(f_1-f_2).$$

The displacement u_z, electric potential ϕ, tangential component of electric field E_x and normal component of electric displacement D_z on the crack surface are given by

$$\begin{aligned}
&u_z(x,0)=-\frac{F_{22}\sigma_l-F_{12}D_l}{F'}\left(a^2-x^2\right)^{1/2}, \qquad \phi(x,0)=-\frac{F_{21}\sigma_l-F_{11}D_l}{F'}\left(a^2-x^2\right)^{1/2},\\
&E_x(x,0)=-\frac{F_{21}\sigma_l-F_{11}D_l}{F'}\frac{x}{\left(a^2-x^2\right)^{1/2}}, \qquad D_z(x,0)=0.
\end{aligned}$$

The energy release rate G^{I} for the impermeable crack model is

$$\begin{aligned}
G^{\mathrm{I}}=-\frac{1}{2F'^2}\Bigg[&\left(F'\sum_{j=1}^{3}\frac{s_j}{\gamma_j}-\sum_{k=1}^{3}h_ks_k\sum_{j=1}^{3}\frac{b_js_j}{\gamma_j}\right)K_{\mathrm{I}}^2\\
&+\left(\sum_{k=1}^{3}h_kt_k\sum_{j=1}^{3}\frac{b_js_j}{\gamma_j}+\sum_{k=1}^{3}h_ks_k\sum_{j=1}^{3}\frac{b_jt_j}{\gamma_j}-F'\sum_{j=1}^{3}\frac{t_j}{\gamma_j}\right)K_{\mathrm{I}}K_{\mathrm{D}}-\left(\sum_{k=1}^{3}h_kt_k\sum_{j=1}^{3}\frac{b_jt_j}{\gamma_j}\right)K_{\mathrm{D}}^2\Bigg],
\end{aligned} \tag{B.9}$$

where $s_j=d_jF_{22}-l_jF_{21}$ and $t_j=d_jF_{12}-l_jF_{11}$. In Equation (B.9) the stress and the electric displacement intensity factors are given by, respectively,

$$K_{\mathrm{I}}=\lim_{x\to a^+}[2\pi(x-a)]^{1/2}\sigma_{zz}(x,0)=\sigma_l(\pi a)^{1/2}, \qquad K_{\mathrm{D}}=\lim_{x\to a^+}[2\pi(x-a)]^{1/2}D_z(x,0)=D_l(\pi a)^{1/2}.$$

Appendix C

The solutions for the open crack model in the infinite piezoelectric material can be derived as follows. The crack face electric boundary condition for the open crack model becomes

$$D_z^+ = D_z^- \quad (0 \le x < a), \qquad D_z^+(u_z^+ - u_z^-) = \epsilon_0(\phi^- - \phi^+) \quad (0 \le x < a), \qquad \phi(x,0) = 0 \quad (a \le x < \infty). \tag{C.10}$$

where the superscripts + and − denote the upper and lower crack surfaces, respectively. By applying the crack face boundary conditions of Equations (A.1) and (C.10), the unknowns $A_j(\alpha)$ in Equations (A.5) are related to σ_l and D_l as follows:

$$\begin{aligned}
&\frac{f_1}{\gamma_1}A_1(\alpha) + \frac{f_2}{\gamma_2}A_2(\alpha) + \frac{f_3}{\gamma_3}A_3(\alpha) = 0,\\
&\frac{1}{\gamma_1}A_1(\alpha) + \frac{1}{\gamma_2}A_2(\alpha) + \frac{1}{\gamma_3}A_3(\alpha) = -\frac{\pi}{2F'}\frac{a}{\alpha}J_1(a\alpha)\big(F_{22}\sigma_l + F_{12}(D_0 - D_l)\big),\\
&\frac{b_1}{\gamma_1}A_1(\alpha) + \frac{b_2}{\gamma_2}A_2(\alpha) + \frac{b_3}{\gamma_3}A_3(\alpha) = \frac{\pi}{2F'}\frac{a}{\alpha}J_1(a\alpha)\big(F_{21}\sigma_l + F_{11}(D_0 - D_l)\big),
\end{aligned}$$

where

$$D_0 = -\epsilon_0\frac{F_{21}\sigma_l + F_{11}(D_0 - D_l)}{F_{22}\sigma_l + F_{12}(D_0 - D_l)}.$$

If $\epsilon_0 = 0$, D_0 is equal to zero. When ϵ_0 becomes very large, the expression for D_0 above shows that $D_0 \to D_l - (F_{21}/F_{11})\sigma_l$.

The displacement, electric potential, tangential component of electric field and normal component of electric displacement on the crack surface are

$$\begin{aligned}
&u_z(x,0) = -\frac{F_{22}\sigma_l + F_{12}(D_0 - D_l)}{F'}\big(a^2 - x^2\big)^{1/2}, \qquad \phi(x,0) = -\frac{F_{21}\sigma_l + F_{11}(D_0 - D_l)}{F'}\big(a^2 - x^2\big)^{1/2},\\
&E_x(x,0) = -\frac{F_{21}\sigma_l + F_{11}(D_0 - D_l)}{F'}\frac{x}{\big(a^2 - x^2\big)^{1/2}}, \quad D_z(x,0) = D_0.
\end{aligned}$$

Energy release rate G^{O} for the open crack model is given by (B.9) with $K_{\mathrm{D}} = (D_l - D_0)(\pi a)^{1/2}$.

References

[Fu and Zhang 2000] R. Fu and T. Y. Zhang, "Effects of an electric field on the fracture toughness of poled lead zirconate titanate ceramics", *J. Am. Ceram. Soc.* **83**:5 (2000), 1215–1218.

[Hao and Shen 1994] T.-H. Hao and Z.-Y. Shen, "A new electric boundary condition of electric fracture mechanics and its applications", *Eng. Fract. Mech.* **47**:6 (1994), 793–802.

[Hwang et al. 1995] S. C. Hwang, C. S. Lynch, and R. M. McMeeking, "Ferroelectric/ferroelastic interactions and a polarization switching model", *Acta Metall. Mater.* **43**:5 (1995), 2073–2084.

[Kalyanam and Sun 2005] S. Kalyanam and C. T. Sun, "Modeling of electrical boundary condition and domain switching in piezoelectric materials", *Mech. Mater.* **37**:7 (2005), 769–784.

[Landis 2004] C. M. Landis, "Energetically consistent boundary conditions for electromechanical fracture", *Int. J. Solids Struct.* **41**:22-23 (2004), 6291–6315.

[McMeeking 1999] R. M. McMeeking, "Crack tip energy release rate for a piezoelectric compact tension specimen", *Eng. Fract. Mech.* **64**:2 (1999), 217–244.

[McMeeking 2004] R. M. McMeeking, "The energy release rate for a griffith crack in a piezoelectric material", *Eng. Fract. Mech.* **71**:7-8 (2004), 1149–1163.

[Narita et al. 2003] F. Narita, Y. Shindo, and K. Horiguchi, "Electroelastic fracture mechanics of piezoelectric ceramics", pp. 89–101 in *Mechanics of electromagnetic material systems structures*, WIT Press, Southampton, 2003. Y. Shindo, ed.

[Narita et al. 2005] F. Narita, Y. Shindo, and K. Hayashi, "Bending and polarization switching of piezoelectric laminated actuators under electromechanical loading", *Comput. Struct.* **83**:15-16 (2005), 1164–1170.

[Park and Sun 1995] S. Park and C.-T. Sun, "Fracture criteria for piezoelectric ceramics", *J. Am. Ceram. Soc.* **78**:6 (1995), 1475–1480.

[Shindo et al. 2002] Y. Shindo, H. Murakami, K. Horiguchi, and F. Narita, "Evaluation of electric fracture properties of piezoelectric ceramics using the finite elementsingle-edge precracked-beam methods", *J. Am. Ceram. Soc.* **85**:5 (2002), 1243–1248.

[Shindo et al. 2003] Y. Shindo, F. Narita, K. Horiguchi, Y. Magara, and M. Yoshida, "Electric fracture and polarization switching properties of piezoelectric ceramic pzt studied by the modified small punch test", *Acta Mater.* **51**:16 (2003), 4773–4782.

[Shindo et al. 2004] Y. Shindo, M. Yoshida, F. Narita, and K. Horiguchi, "Electroelastic field concentrations ahead of electrodes in multilayer piezoelectric actuators: experiment and finite element simulation", *J. Mech. Phys. Solids* **52**:5 (2004), 1109–1124.

[Shindo et al. 2005] Y. Shindo, F. Narita, and M. Mikami, "Double torsion testing and finite element analysis for determining the electric fracture properties of piezoelectric ceramics", *J. Appl. Phys.* **97** (2005), 114109.

[Sun and Achuthan 2004] C.-T. Sun and A. Achuthan, "Domain-switching criteria for ferroelectric materials subjected to electrical and mechanical loads", *J. Am. Ceram. Soc.* **87**:3 (2004), 395–400.

[Sun and Park 2000] C. T. Sun and S. B. Park, "Measuring fracture toughness of piezoceramics by vickers indentation under the influence of electric fields", *Ferroelectrics* **248** (2000), 79–95.

[Wang and Mai 2003] B. L. Wang and Y.-W. Mai, "On the electrical boundary conditions on the crack surfaces in piezoelectric ceramics", *Int. J. Eng. Sci.* **41**:6 (2003), 633–652.

[Xu and Rajapakse 2001] X.-L. Xu and R. K. N. D. Rajapakse, "On a plane crack in piezoelectric solids", *Int. J. Solids Struct.* **38**:42-43 (2001), 7643–7658.

[Yoshida et al. 2003] M. Yoshida, F. Narita, Y. Shindo, M. Karaiwa, and K. Horiguchi, "Electroelastic field concentration by circular electrodes in piezoelectric ceramics", *Smart Mater. Struct.* **12** (2003), 972–978.

Received 16 Jun 2006. Revised 13 Apr 2007. Accepted 20 Apr 2007.

YASUHIDE SHINDO: shindo@material.tohoku.ac.jp
Department of Materials Processing, Graduate School of Engineering, Tohoku University, Aoba-yama 6-6-02, Sendai 980-8579, Japan

FUMIO NARITA: narita@material.tohoku.ac.jp
Department of Materials Processing, Graduate School of Engineering, Tohoku University, Aoba-yama 6-6-02, Sendai 980-8579, Japan

FUMITOSHI SAITO: *Department of Materials Processing, Graduate School of Engineering, Tohoku University, Aoba-yama 6-6-02, Sendai 980-8579, Japan*